Journal of Power Sources 195 (2010) 5452–5467

Contents lists available at ScienceDirect

Journal of Power Sources

journal homepage: www.elsevier.com/locate/jpowsour

Review

Durability of Ni anodes during reoxidation cycles

M. Ettler[a,*], H. Timmermann[b], J. Malzbender[a], A. Weber[b], N.H. Menzler[a]

[a] Forschungszentrum Jülich GmbH, Institute of Energy Research IEF, 52425 Jülich, Germany
[b] Institut für Werkstoffe der Elektrotechnik IWE, Karlsruhe Institute of Technology KIT, 76131 Karlsruhe, Germany

ARTICLE INFO

Article history:
Received 13 October 2009
Received in revised form 11 March 2010
Accepted 14 March 2010
Available online 19 March 2010

Keywords:
Solid oxide fuel cell
Anode
Reoxidation
Redox cycling
Degradation

ABSTRACT

Anodes manufactured from NiO- and yttria-stabilized zirconia (Y_2O_3 doped ZrO_2, YSZ) powders are today's state of the art for solid oxide fuel cells (SOFCs) because they are easy to manufacture and have high performance in both anode-supported and electrolyte-supported cells. However, such cells can show significant degradation or fail completely if nickel is reoxidized during high-temperature operation even though it can be reduced again. Tests with stacks and systems have shown that system shutdown procedures, accidental air entry due to component failure or controlled air feed to the anode side as a result of operational necessities may occur and result in the reoxidation of the metallic nickel. This reoxidation is not only associated with a volume expansion, but also with significant structural changes in the anode microstructure, generating stresses in the anode itself, as well as in the electrolyte. These stresses can exceed the stability of the components, potentially promoting crack growth, which leads to degradation of the SOFC or complete failure.

This problem has been addressed by a number of contributions in the literature over the last decade, but interest is increasing, particularly because SOFC systems are being discussed for transport and mobile applications requiring new system specifications. The most critical problem to be overcome is the tolerance of a large number of intentional redox cycles due to system requirements during operating lifetime.

This article gives an overview of the various approaches to the redox problem by summarizing many of the contributions, starting with a basic understanding of the underlying physicochemical processes of Ni reduction and oxidation and ending at stack-level results, leading finally to their combination with recent findings. It aims to elaborate reliable results and open questions on this topic considering the mechanical and electrochemical aspects of the problem.

Contents

* Corresponding author. Tel.: +49 2461 616162; fax: +49 2461 612455.
E-mail addresses: m.ettler@fz-juelich.de (M. Ettler), j.malzbender@fz-juelich.de (J. Malzbender), andre.weber@iwe.uni-karlsruhe.de (A. Weber), n.h.menzler@fz-juelich.de (N.H. Menzler).

0378-7753/$ – see front matter © 2010 Elsevier B.V. All rights reserved.
doi:10.1016/j.jpowsour.2010.03.049

1. Introduction

As long as fuel (e.g. hydrogen, reformate or a methane/water vapour mixture appropriate for internal reforming) is supplied to the anode side of the cell during SOFC operation, the nickel in the anode substrate and anode layer remains in the reduced state. However, if this fuel supply is interrupted, oxygen will still diffuse from the cathode side through the electrolyte to the anode side or enter via imperfect seals from outside the system or the BoP (balance of plant) components (e.g. reformer, afterburner). Interruption of the fuel supply may occur accidentally as a result of an error in the system control or intentionally upon system shutdown. The presence of oxygen on the anode side of the cell, especially at typical operation temperatures for SOFCs, will lead to reoxidation of the nickel. Operation with undesirably high fuel utilization can also cause the oxygen activity to rise above the equilibrium condition between Ni and NiO and form NiO [1]. The reoxidized nickel can be re-reduced, but various investigations have revealed that the structure of substrate and anode cannot be restored [2–8]. The structural changes in the substrate and anode upon reoxidation lead to dimensional changes that generate stresses in substrate, anode and other cell components, potentially promoting damage in all layers of the cell and therefore degrading cell performance or even causing complete failure of the cell [1,3,5,6,9,10].

Investigations of the redox tolerance of Ni-based SOFC anode substrates and anodes have gained increasing interest since SOFC systems are not only being discussed as solutions for future stationary small-scale domestic, residential and industrial power generation, but also for transport and mobile applications, e.g. as auxiliary power units in aircraft, trucks and cars [11].

In the literature, several "system solutions" for avoiding reoxidation of substrate and anode are discussed with particular emphasis on fuel gas supply interruption during system shutdown: e.g. maintenance of fuel gas supply until the system temperature falls below a critical temperature, inert purge gas supply for the shutdown procedure, cell reversal or "passive solutions" such as hydrides, oxygen getters or steam purging. In real fuel cell power systems emergency (shut down) procedures, eventually including inert gas purging, have to be implemented in the control system and they automatically start in case of accidental failures. They are needed to comply with safety standards, but they may be also useful to protect the electrochemical module from further damages [9,12].

In order to achieve a breakthrough on the market, SOFC systems have to hit very tight cost targets. Therefore the application of expensive "system solutions" is undesirable. Moreover, some of these solutions only provide an answer for the intentional interruption of the gas supply, but not for accidental operation failure. Therefore it is desirable to find a technological solution, i.e. to prevent the damage caused by this oxidation in order to achieve tolerance of reduction–reoxidation sequences (redox cycles). Furthermore, if the SOFC is used as an auxiliary power unit (APU) for vehicle systems, solutions based on additional components should be avoided due to additional weight and complexity. In addition to considerably tightened design requirements, mobile applications for SOFC systems also have to tolerate a large number of intentional redox cycles in the case of system shutdown during operating lifetime, because "system solutions" are even less probable in mobile than in stationary applications.

2. Current state of knowledge

A number of investigations in the literature aimed to describe the reoxidation process in substrates and anodes and the resulting structural and dimensional changes causing damage in the cell. The following section gives an overview of the basic processes governing the reduction and oxidation of nickel, the observed processes in the substrate and anode upon redox cycling, the associated mechanisms and their consequences for other cell components. Furthermore, approaches and their underlying concepts for a technological solution to the redox problem proposed in the literature are outlined.

2.1. Reduction of NiO

The reduction of NiO particles in H_2 begins with an induction period. During this period, nucleation of metallic clusters takes place. These clusters then grow into crystallites at an approximately linear rate [1]. Radovic et al. [13] showed that the initial reduction causes a negligible change in the bulk dimensions of the cermet. The volume decrease associated with a change from NiO to Ni induces an increase in cermet porosity. The reduction continues at the interface between NiO and the previously reduced porous nickel. At temperatures between 200 and 600 °C, the reaction rate is rapid and interface controlled with an activation energy of 85–90 kJ mol^{-1}. At higher temperatures, sintering of the porous nickel takes place, which restricts the access of H_2 to the oxide–metal interface [14,15].

2.2. Reoxidation of nickel

In the temperature region typical for SOFC startup and operation (300–800 °C), it has been shown that the dominant mass-transport process governing NiO film growth is the outward diffusion of nickel ions along dislocations and grain boundaries in the NiO layer [16,17]. In this region the activation energy has been determined as about 144 kJ mol^{-1} and the rate constant k_p at 800 °C in the range of 10^{-11} and 10^{-12} cm^2 s^{-1} [17–19]. Estimates on the basis of these data show that a 1-μm-thick film of NiO is formed in 4 min [1]. Anode oxidation at high temperatures is thus a potentially fast process. The Wagner theory predicts that k_p is dependent on the oxygen partial pressure ($k_p \propto (p_{O_2})^{1/6}$) [20]. Hence, if the oxygen partial pressure is low, the growth rate is reduced.

The process of outward nickel ion transport for oxide film growth leads to a potential problem in maintaining contact at the metal–oxide interface. When interface recession is inhibited, the NiO layer also grows via the inward transport of oxygen, probably by gas molecule permeation through fissures in the oxide scale [21]. This applies particularly to the oxidation of small nickel parti-

cles as they are found in the substrate and anode of a SOFC. For them, the outward-growing, almost spherical oxide layer is too rigid for the interface recess [1]. Karmhag et al. [22,23] investigated the oxidation of nickel particles of various sizes. Studies on small polycrystalline nickel particles of around 5 μm in diameter showed that the activation energy is independent of the morphology and surface structure of the particles. The measured parabolic rate constants fall within the range typical of bulk nickel oxidation. As the metal core is exhausted, the oxidation kinetics deviates from the parabolic behaviour.

2.3. Nickel/YSZ cermets

Although nickel oxidation and reduction have been well investigated, these results cannot be applied directly to nickel-based substrates and anodes because of their composite structure with YSZ as ceramic component. Redox cycling on nickel-based cermet substrates and anodes for SOFCs has been studied by testing bars, discs and powders [2–4,10,24–27]. Changes in weight, dimensions, mechanical integrity and microstructure have been investigated using thermogravimetry, dilatometry and microscopy.

Experiments on fully dense rectangular bars (60 vol.% NiO) in N_2/10% H_2 and air in the temperature range of 600–800 °C showed linear reduction kinetics, indicating an interface-controlled mechanism with an activation energy of 94 kJ mol^{-1} [24]. This is consistent with the activation energy found for the reduction of single particles [14,15]. The reoxidation kinetics, however, were found to be parabolic and diffusion controlled. The rate-determining step appeared to be the diffusion of oxygen through the pores, as the effective diffusion coefficient (estimated to be $\sim 10^{-7}$ cm^2 s^{-1}) was independent of temperature and oxidation was not uniform [24]. At 550–650 °C Stathis et al. [25] and at 700–800 °C Modena et al. [26] found a logarithmic behaviour, suggesting that nickel diffusion through the growing NiO layer was the rate-determining step for oxidation in air. This difference is probably caused by the much higher porosity of the samples compared to those used by Tikekar et al. [24]. Investigating redox behaviour with cermet anodes (57 wt.% NiO), Waldbillig et al. [4] found a linear law for reduction and a parabolic law for reoxidation at temperatures below 700 °C and low degrees of conversion. At higher temperatures between 700 and 850 °C, a divergence from parabolic behaviour was found. The activation energies reported were 78 and 87 kJ mol^{-1} for reduction and reoxidation, respectively. The activation energy is therefore slightly lower than for single nickel particles, which could be a result of gas transport in the pore structure of the cermet (diffusion through pores). A comparison of the redox kinetics of Ni/YSZ cermets and pure nickel powder showed a stronger temperature dependence of the oxidation and a weaker temperature dependence of the cermet reduction [8,27].

2.3.1. Effect of reoxidation

As discussed above, a number of studies indicated that reduced nickel-based substrates and anodes do not return to their initial state upon reoxidation. For example, Cassidy et al. [28] found a significant volume increase after reoxidation compared to the initial state. The suggested explanation was sintering and coalescing of finely distributed NiO particles during reduction into a coarser network of larger particles. Consequently, the local volume change upon reoxidation becomes too big to be compensated by the local porosity. Klemensø et al. [3] proposed a simple model for the mechanism behind redox instability on the basis of experimental observations at 1000 °C [2]. They associated the irreversible behaviour with the rounding of nickel particles during structural reduction and reorganization during reoxidation depending on the initial microstructure and oxidizing temperature. The model was improved using DC conductivity measurements to characterize the microstructural changes in Ni–YSZ cermets upon redox cycling. It suggests that the reorganization of the Ni/NiO phase during reduction and reoxidation accounts for the redox instability of the anode and that the oxide growth causes damage to the YSZ network, but that it may promote an improvement in the percolating Ni/NiO network up to a critical value for the porosity [29]. Waldbillig et al. [5] ascribed the structural changes to the formation of a large number of intergranular pores after reduction. These pores provide many nucleation sites for the NiO grains to form and thus promote the formation of small randomly orientated grains. This grain refinement finally causes the creation of a spongy microstructure of NiO with a much bigger volume than the initial state. All of these mechanisms suggest that the initial microstructure before the first reduction significantly influences the redox behaviour. This was confirmed recently in experiments by Pihlatie et al. investigating the dimensional behaviour of Ni/YSZ composites during redox cycling [10].

2.3.2. Influence of the microstructure

A number of groups have investigated the influence of the microstructure on the redox behaviour and have proposed potential solutions for the redox problem by adjusting various parameters. Fouquet et al. [30] studied linear dimensional changes by dilatometry with respect to sintering temperatures and particle sizes. They found no length change during initial reduction and better dimensional redox stability for samples sintered at lower temperatures. It was suggested that the material is more porous to accommodate volume changes upon reoxidation when it is sintered at lower temperatures. Malzbender et al. [6] argued from the thermoelastic point of view that higher porosity should be beneficial for redox tolerance of substrate and anode. Smaller initial NiO particles and a finer microstructure were found to be advantageous for redox stability in experiments by Fouquet et al. [30]. In a study by Pihlatie et al., dilatometry measurements revealed that dimensional stability is dependent on microstructure and that samples with a high porosity were most stable [31]. However, a study by Waldbillig et al. [4] concerning the differences in redox behaviour between substrate and anode with coarse (substrate) and fine (anode) microstructures at 750 °C yielded no significant volume change during either reduction or reoxidation of the samples with a coarse structure, whereas the samples with a fine microstructure increased in volume by 0.9–2.5% and cracked after reoxidation. The suggested explanation is better redox tolerance in the samples with a coarser structure due to bigger pores. The results of Fouquet and Waldbillig are thus inconsistent with respect to fine or coarse microstructure. Klemensø et al. [3] investigated the effect of the yttria content in the YSZ component and concluded that the chosen YSZ powder has a major influence on redox stability with 3 mol% Y_2O_3 doped ZrO_2 (3YSZ) powders having significantly lower expansion rates compared to 8 mol% Y_2O_3 doped ZrO_2 (8YSZ) powders. Pihlatie et al. pointed out that redox cycling leads to a decrease in Young's modulus. They believe that the loss of stiffness could be correlated with the cumulative redox strain, measured from the macroscopic sample length change with mechanical degradation, due to damage starting at about 0.5% strain (dL/L_0) and a macroscopic loss of integrity resulting from strain exceeding 2.5% [32].

Parametric studies on the effect of substrate composition and microstructure comparing various fine/coarse YSZ ratios, NiO particle sizes and content, as well as sintering temperatures revealed high oxidation strain but negligible irreversible strain for high NiO content. High fine/coarse YSZ ratios gave high and irreversible oxidation strain. A high sintering temperature resulted in a rather rigid structure showing hardly any reduction strain [33]. The authors concluded that there is an optimum composition and microstructure for substrates and anodes which yield a minimum redox strain and lead to mechanical degradation. Considering the various approaches in this field and to some extent inconsistent results, fur-

ther investigations on optimizing the microstructure are required [1,9]. The influence of particle sizes, particle size ratios, porosity, and pore size distribution and composition on the redox tolerance of substrates and anodes has yet to be clarified as does the potential for a technological solution of the redox problem by optimizing the microstructure. However, the investigations show that these parameters determine the behaviour of substrates and anodes upon reoxidation by influencing parameters such as tortuosity, diffusivity and/or permeability.

2.3.3. Influence of the reduction and reoxidation temperature

The reduction and reoxidation temperature also has a strong impact on the performance and redox stability of the cell. Grahl-Madsen et al. [34] have shown an almost linear relationship of the electrical conductivity between room temperature, and reduction temperature. Substrates reduced at 1000 °C had twice the conductivity of those reduced at 800 °C. This could be due to enhanced nickel sintering at higher temperatures improving percolation. Since the conductivity of substrates reduced at lower temperatures could not be improved significantly by additional heat treatment at higher temperatures, the nickel network formation obviously involves simultaneous reduction and sintering. Pihlatie et al. [10] showed that the reduction temperature has a significant impact on the macroscopic strain caused by redox cycling. Higher strain was found in samples reduced at higher temperatures. However, this can also be ascribed to sintering effects during reduction at high temperatures leading to a coarser microstructure than samples reduced at lower temperatures. In the same study, the dependence of the macroscopic strain caused by redox cycling on reoxidation temperature was found to be even stronger than on reduction temperature. Tests on electrochemical performance also revealed that redox cycling at lower temperatures (650 °C) is advantageous compared to redox cycling at higher temperatures (850 °C) as smaller Ni grains and an undamaged ceramic structure were observed in the anode [31]. In agreement with this study, oxidation experiments at temperatures between 550 and 950 °C by Stathis et al. [25] showed that with increasing oxidizing temperatures the macroscopic strain increases, showing values from 0.27% at 650 °C to 0.54% at 800 °C. It would appear that the higher the oxidation rate, the larger the observed bulk volume expansion. The great influence of the oxidizing temperature with a tendency towards larger volume change and higher strain leading to severe damage at higher temperatures was also observed in studies by Waldbillig et al. [4], Zhang et al. [7] and Klemensø et al. [2,3].

2.3.4. Mechanisms leading to cell damage and failure

Redox cycling results in microstructural changes in the substrate and anode and significant volume expansions as discussed above, but it does not necessarily lead to complete failure of a cell. Some investigations on cells and half-cells (substrate–anode–electrolyte assemblies) provided deeper insights into the mechanisms that cause damage in cell components other than the substrate and anode, which potentially leads to complete disruption and failure of the cell. The substrate and anode expand upon reoxidation, whereas electrolyte and cathode layers cannot keep up with this expansion. Tensile stresses arise in the cell. If the tensile residual stresses in the electrolyte exceed its tensile strength, cracks form in the electrolyte [4–6,25,28,31,35–41]. Stresses, curvature and cracking are strongly dependent on homogeneity of oxidation and the degree of oxidation (DoO) [4–6,25,36,38–40], which are defined as the ratio between the mass of oxygen absorbed by the substrate and the maximum mass of oxygen the substrate would have been able to absorb upon complete oxidation ($DoO = m_{oxy}(absorbed)/m_{oxy}(max)$). Both homogeneity and DoO also strongly depend on the oxidizing conditions, e.g. temperature, time of oxidation and gas flow [36,39,40]. Malzbender et al. [6,38] monitored the development of the curvature of cells during redox cycling. The results showed an inhomogeneous reoxidation at 800 °C in air leading to complicated stress distributions ultimately resulting in electrolyte cracking. They also reported that reoxidation initially produced a bending towards the electrolyte. After some time, however, the change in curvature was reversed. This was explained by a reoxidation front that proceeded from the free surface of the anode substrate towards the electrolyte and a local change in elastic modulus in the anode support with progressing reoxidation. Formation of reoxidation fronts could be observed in investigations on areas where reoxidized half-cells fractured. This shows that the progress of the reoxidation front strongly depends on the reoxidation temperature and therefore is a potential explanation for the differences in the behaviour of the cell upon reoxidation at different temperatures [39,40]. In another approach by Faes et al., creeping effects in the anode support during reoxidation were found to be the reason for cell warpage upon reoxidation. Reoxidation strain was investigated on half-cells based on 250-μm tape-cast Ni–YSZ cermet substrates with a 4-μm-thick 8YSZ electrolyte by crack width measurements in the electrolyte and porosity measurements inside the anode support. It was found that anode strain is strongly dependent on the temperature at which redox cycling occurs and 550 °C was calculated and validated as a "safe" redox temperature. In other words, the reoxidation strain will not cause electrolyte cracking at that temperature. Furthermore, successive redox cycling was found to induce an irreversible process. However the maximum strain appears to reach a maximum value after approx. 10 cycles. Faes et al. also state that from porosity measurements it is possible to estimate the number of redox cycles endured by a cell tested in stack conditions, depending on the location inside the cell. The limit for reoxidation strain was determined in the range of 0.12–0.21% based on finite element modelling and failure statistics in dependence on redox temperature and sample size for a constant thickness [41].

There are only a few studies on the redox behaviour of complete cells with respect to electrochemical and performance tests. Cassidy et al. [28] observed a drop in open circuit voltage (OCV) from 0.85 to 0.4 V due to significant cracking of the electrolyte after a redox cycle. Mueller et al. found that in case of electrolyte-supported cells, the electrolyte substrate is not affected by redox cycling. Nevertheless, a severe increase in polarization resistance of 3–12% per redox cycle was observed at an operating temperature of 950 °C. In redox tests on Sulzer cells [37], the substrate remained undamaged while the electrolyte and cathode were impaired, causing an OCV drop from 990 to 850 mV. In attempts to optimize substrate characteristics, the OCV drop was reduced significantly for substrates with low fine/coarse YSZ fraction ratios and a high NiO fraction. In this unsealed design, cracks in the electrolyte were now concentrated only at the periphery of the cell. As substrates with this composition exhibited the lowest irreversible oxidation strain in dilatometry, this parameter was proposed as the major factor in optimizing microstructure to improve redox stability.

Waldbillig et al. [5] demonstrated that their cells even survived complete reoxidation at 750 °C without catastrophic losses in electrochemical performance. This could also be associated with a low oxidation strain. The actual loss in cell performance increased with the extent of oxidation (time of oxidation varying the DoO) and the number of cycles, and was attributed to tensile cracking of the electrolyte. Furthermore, they had some success in improving redox tolerance by introducing a gradation in nickel content in the anode and a second similar layer on the opposite face of the substrate to restrict ingress of oxygen from the gas phase [42].

Finally Holtappels et al. [43] performed redox tests on a three-cell stack (Sulzer Hexis design) fabricated by die cold pressing of the substrate and spray pyrolysis of the electrolyte. A rapid drop in OCV was measured after one redox cycle for two of the three cells. In

the third cell, the OCV remained unchanged and the area-specific resistance (ASR) decreased. The improved cell had a coarser YSZ microstructure in the substrate and anode, potentially explaining the poorer electrochemical performance but better redox stability.

3. Reoxidation–fracture

> "The cell structure in a working SOFC stack is subject to mechanical loads from a variety of sources, many of which depend on the details of the cell and stack design. For example, the interconnectors and bipolar plates will impose strains that depend on their thermal expansion coefficients and the compliance of constraints imposed by seals. In addition the cell layers are likely to be under residual stress resulting from cooling from the manufacturing process and initial reduction of the anode. Whether these persist at the operating temperature, or are gradually relaxed by creep is not known. . .. Furthermore, a real cell will not be isothermal and this will generate additional stresses." Sarantaridis and Atkinson [1].

In the subsequent section, the mechanical effects associated with reoxidation are reviewed with respect to macroscopic and microscopic effects and possibilities of mechanical modelling.

3.1. Macroscopic effects

3.1.1. Strength

The relationship between reoxidation and fracture strength has received limited attention in the literature [25,44]. Although the strength of the substrates appears to be only slightly influenced by the initial reduction [34,44], reoxidation can cause spontaneous mechanical failure, especially at high reoxidizing temperatures [25]. This implies that the associated strain is temperature dependent. However, specimens reoxidized in air below 650 °C showed an increase in bending strength, which can be attributed to a porosity reduction. In agreement with this, Mohammadi et al. recently reported [45] that after reoxidation cycles the maximum strength of the reoxidized anode was higher than in reduced state.

3.1.2. Expansion and warping

Whereas the macroscopic dimensions of cells do not appear to be changed by reduction [28], reoxidation leads to significant alterations due to the irreversible structural change in NiO. Some authors have measured the volume change with dilatometers [3,4,10,25,28] and have shown that the magnitude of expansion depends strongly on parameters such as initial porosity, nickel content [4] and the oxidation rate of the composite, and therefore the reoxidation temperature [10,30]. It has been reported that the magnitude of the irreversible change in NiO after reoxidation depends on the actual particle size (3–9%, [28]). Furthermore, Robert et al. [33] stated that initial reduction led to a contraction of approximately 0.15%, while the reoxidation expansion accounted for 0.35%. A second reduction gave a contraction of approximately 0.25% leaving a permanent irreversible elongation of approximately 0.1%. It was observed by Sarantaridis et al. [46] that the first reoxidation cycle resulted in a strain of 0.14%, and a second reoxidation increased the strain by additional 0.6%. Pihlatie et al. [10] reported that the cumulative redox strain after three redox cycles increases from 0.25% to 3.2% dL/L_0 when the isothermal redox cycling temperature is increased from 600 to 1000 °C. Recently, Laurencin et al. [47] performed reoxidation tests at 800 °C with free standing, i.e. unconstrained, cells fabricated by Forschungszentrum Jülich based on a 1.5-mm anode substrate. In this study, the critical degree of reoxidation was found to be in the range of 58–71%, leading to an oxidation strain in the range of 0.26–0.34%. In approaches using mechanical modelling to predict the critical oxidation strain, somewhat lower values of 0.19% were calculated for the energetic approach and 0.16% for the probabilistic approach. This corresponds to a critical degree of oxidation of about 50%. A possible explanation for the discrepancies between the predicted and measured values is that inappropriate material data was used for the calculations due to a lack of more reliable values. In the same study, the impact of reoxidation induced by ionic current (electrochemical reoxidation) was observed. Evaluation of impedance diagrams and observations in post-test analysis revealed that delamination at the substrate/anode or anode/electrolyte interface is the major failure mechanism for this type of reoxidation. Experiments and a mechanical analysis for the scenario in which only the anode (not the substrate) is reoxidized suggest that substrate/anode interface delamination is more likely to occur as this interface was found to be weaker than the anode/electrolyte interface [48].

Klemensø et al. [49] measured the reoxidation expansion of the specimen characteristics of an anode support and an anode layer for an anode substrate containing 3YSZ and 8YSZ, and found that the anode support structure displayed significantly lower expansion. In addition, it has been reported that a reduction in the sintering temperature decreases the reoxidation expansion by virtue of the lower porosity-related stiffness [30]. Hence, reoxidation strain was suggested to be a major factor in controlling reoxidation stability [37]. Crack formation within the anode has been associated with an increase in polarization resistance [30]. Different reports on the reoxidation of anode-supported cells have revealed electrolyte cracking [28,37]. In fact, cracking was more pronounced at 750 °C than at 600 °C [30].

Interrupted oxidation experiments on anode supports revealed irreversible linear strain behaviour with reversible behaviour for the elastic modulus, indicating that uniform oxidation caused no substantial damage in the anode support [1]. Interrupted oxidation on free-standing cells resulted in failure by extensive electrolyte channel cracking at a critical degree of oxidation of ~50%. Electrochemical oxidation of cells incorporated in a metal housing, on the other hand, led to anode support cracking at only ~5% oxidation. The cracking patterns in the latter case were consistent with tensile cracking in the outer regions of the substrate driven by an oxidation-induced expansion of the inner region. A model of cell stability has been developed in which oxidation occurs preferentially within a central zone. This model predicts tensile cracking of the substrate at much lower values of the degree of oxidation compared to uniform oxidation, which is in good agreement with the experimental observations. It was concluded that non-uniform oxidation processes will have more detrimental effects than uniform ones, and are also likely to occur in the case of leakage in seals or at high fuel utilization [46].

In general, depending on the cermet producer, the size of the Ni/YSZ particles in the reduced cermet was in the order of a few micrometers. It has been shown that in the case of reoxidation the particles increase in size with a sponge-like microstructure, which leads to strains because the porosity is limited. Even in the case of slow reoxidation, fracturing was observed of the electrolyte and microcracks in the anode [6]. In addition, nickel sintering and coarsening has been reported for high-temperature reoxidation (~1000 °C [48]). However it is unclear whether these processes occur and influence the behaviour at the usual operating temperature of ~800 °C [36]. In fact, current developments aim at even lower operating temperatures of 600 °C to reduce the material requirements [50].

In contrast to the macroscopic dimensions, the curvature of cells increased significantly during both reduction and reoxidation. The curvature and curvature change increased with decreasing substrate thickness [51]. An increase in curvature resulting from reoxidation has also been reported in [35]. Although creep can occur during cooling from the sintering temperatures, the elec-

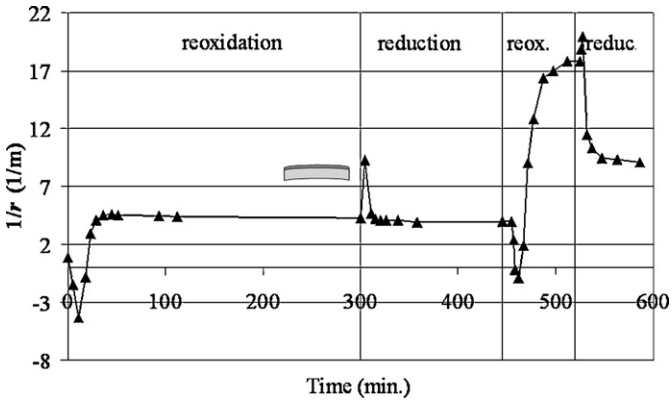

Fig. 1. Curvature during reoxidation and re-reduction (0.27 mm anode, 800 °C).

trolyte is in a state of compression and the anodes tend to be in a state of tension due to the difference in thermal expansion coefficients [52]. The elastic energy represented by the residual stress is conserved during the reduction process as long as relaxation/creep processes are negligible. Hence, as a result of the lower stiffness of the Ni/YSZ cermet compared to the NiO/YSZ structure the curvature increases. While the change in curvature during reduction is a result of the change in cermet stiffness, the change in curvature during reoxidation is closely related to the irreversible expansion of Ni during transformation into NiO. During reoxidation, the curvature changes with time first in the opposite direction and then back to the initial direction. Note that, the results presented in all figures are based on cells with Ni content 40%, porosity 30–40%.

The final curvature is larger than in the initial oxidized state, although reoxidation expansion should lead to a reduction in curvature (Fig. 1). Additional reduction/reoxidation cycles increase the curvature further.

A model has been proposed [51] to interpret this complex warping behaviour where reoxidation starts at the free surface of the anode and then continues until the entire anode is reoxidized. The expansion of the reoxidized substrate, which starts at the free substrate surface, initially changes the curvature to the opposite direction. Once the reoxidized area has passed the neutral axis, the expansion causes a moment in the opposite direction, changing the curvature again to the opposite direction. A similar explanation holds for the curvature change during reduction. The proposed process, however, does not explain why the curvature is larger in the reoxidized than in the initial oxidized state. It was proposed that this is related to a decrease in anode support stiffness, which could be due to microcracks which were observed in the anode substrate [6,51].

Ettler et al. have reported that reoxidation at 800 °C leads to larger warping than at 700 °C, which was associated with a larger reoxidation strain [36]. On the basis of these investigations, the following dominant failure mechanism was suggested. Upon reoxidation, the substrate expands starting from the free surface of the anode substrate. The electrolyte cannot follow this expansion, and tensile stresses arise. At first, these stresses can be relieved by warpage of the cell. Once the tensile residual stresses in the electrolyte exceed the tensile strength, cracks form in the electrolyte. The degree of reoxidation (DoO) and homogeneity of oxidation determine the warpage and cracking of the cell. The more homogeneous the reoxidation is the lower the warpage, the higher the tolerable DoO and the better the reoxidation stability of the cell. In the case of samples attached to steel plates or brazed in a metallic frame, sealant delamination and cell cracking was observed as a result of cell warpage upon reoxidation.

3.1.3. Residual stress

The overall room temperature residual stress in the electrolyte of a 1.5-mm-thick cell determined using X-ray diffraction (XRD) was about −560 MPa for an oxidized anode substrate and −520 MPa for a reduced anode substrate [53]. Hence, the electrolyte is under compressive stress. Cells with slightly different anode geometry (2 mm) and electrolyte thickness (~20–40 μm) gave rise to stresses in the same order of magnitude (−660 MPa for oxidized, −670 MPa for reduced cells [54]). With respect to high-temperature diffraction studies, it has been reported that the residual stress decreases by a factor of 6–8 for oxidized cells and 4–6 for reduced cells at operating temperature [55,56]. For reoxidized cells, it has been reported that the residual stress in the electrolyte layer is ~60% lower than in the initial oxidized state and ~30% lower than in the reduced state [55]. In another study, the internal stresses for samples consisting of a 300-μm anode (made of NiO and 3YSZ in the tetragonal phase) and a 20-μm 10 mol% scandia-stabilized zirconia (10 mol% Sc_2O_3 doped ZrO_2, 10ScSZ, in the cubic phase) electrolyte were measured in situ during reduction and reoxidation cycles using high-energy X-ray synchrotron radiation of about 70 keV [55,57]. At room temperature, the electrolyte has a compression of about 400 MPa and the anode a tension of 50–100 MPa. During heating and reduction, the compressive stress in the electrolyte decreases and becomes approximately zero at 1000 K. Due to the lower coefficient of thermal expansion (CTE) of the anode after reduction compared to the as-sintered state, the compressive stress of the electrolyte reaches only about 200 MPa after cooling back down to room temperature in the reduced state. During reoxidation, the Ni phase disappears at about 800 K, at which point the internal stress in the electrolyte changes into tension. This tensile stress is the reason for electrolyte cracking upon reoxidation.

Recently, XRD measurements at room temperature were carried out on specimens in the as-sintered, reduced and reoxidized state. Reoxidation temperature and DoO were varied in these investigations. Typical results obtained at 600 and 800 °C are shown in Fig. 2.

As the reoxidation front proceeds towards the electrolyte, additional compressive stresses arise as long as the reoxidation front has not passed the neutral axis of the composite. However, it has to be taken into consideration that the stress in this study was measured at room temperature and hence is also strongly influenced by the difference in thermal expansion of the reoxidized and still reduced volume. In fact, the stress in the reoxidized state is slightly reduced or nearly equal to the value of the reduced specimen. In addition, the specimens showed an increase in curvature. If the reoxidation strain in the substrate is neglected (see also [3]), the stress in the electrolyte should be between the value for the oxidized and reduced state. The fact that the stress is even lower than in the reduced state might be the result of differences in thermal expansion, creep or microfracture in the substrate or at the interface between reoxidized and reduced material (Fig. 3).

3.2. Microscopic effects

In order to obtain further insight into the reoxidation process, micrographs were taken from exactly the same location of an anode-supported half-cell ranging from the co-fired state to the status after the second reoxidation [58]. The initially dense NiO particles (Fig. 3a) show shrinkage upon reduction (Fig. 3b). However, the microstructure after reoxidation is different from the initial as-prepared microstructure. The particles are fragmented in the reoxidized state and have a spongy microstructure (Fig. 3c). The reoxidized particles have a greater porosity (~30%) and occupy a larger volume than in the as-prepared state. Furthermore, microcracks in the anode and electrolyte are visible after reoxidation (Fig. 3c). Reducing the NiO again results in dense particles (Fig. 3d),

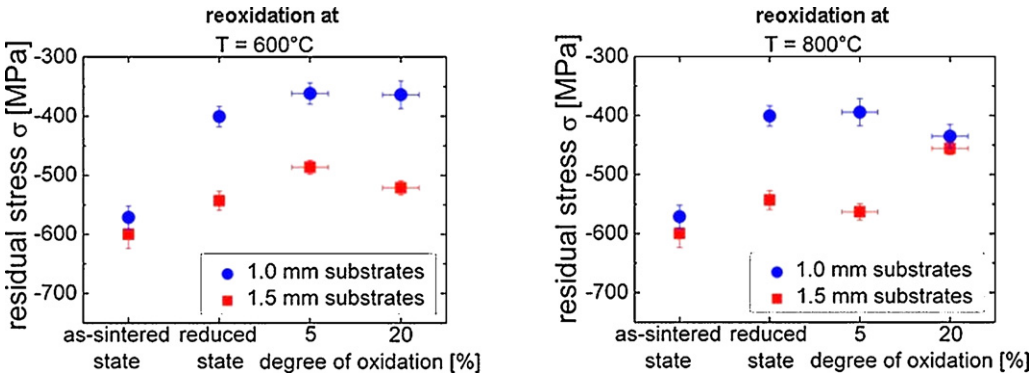

Fig. 2. Relationship between residual stress and degree of reoxidation (XRD measurement at room temperature) for reoxidation temperatures of 600 °C (left) and 800 °C (right)

which appear to occupy a larger volume than in the initial reduced state (Fig. 3b) and hence display a coarser structure. After the second reoxidation, the NiO particles appear to be even more fragmented, showing again the spongy microstructure (Fig. 3e). The electrolyte crack shows a larger opening. Macroscopically, the crack density was larger after the second reoxidation than after the first. This could be the result of the coarser structure of the Ni in the re-reduced state. Additional TEM investigations also revealed the increased porosity in the reoxidized NiO particles [58].

3.3. Mathematical descriptions

The material expansion related to anode reoxidation causes global tensile stresses in the electrolyte. By comparing the electrolyte strength with thermal and reoxidation stresses obtained using FEM simulations, fracture has been predicted for anodic expansions between 0.16–0.19% and 0.12–0.15%, respectively [47,59].

A simple elastic and brittle fracture description of the mechanical effects of reoxidation cycling has been developed for planar, unconstrained cells and cells that are constrained to remain flat [1]. Key parameters in the analysis were the reoxidation strain and the elastic modulus of the anode in its oxidized state. Three characteristic cell configurations were considered: anode-supported, electrolyte-supported, and inert-substrate-supported [1]. The dominant structural layer in each configuration is perfectly rigid and experiences zero elastic strain. The driving force for failure was the release of elastic energy stored within the stresses in the system, which was induced by the tendency of the anode to expand upon oxidation. The necessary, but insufficient, condition for failure was an energy balance for steady-state crack extension.

It was concluded that oxidation expansion should be below about 0.1% to avoid tensile cracking of the electrolyte. For electrolyte-supported cells, the failure mode is likely to be compressive delamination (spalling) of the anode from the electrolyte. This failure mode can be initiated at an edge or by buckling. The inert-substrate-supported design is also likely to fail by compressive delamination—this time at the interface between the anode and substrate. However, in this case, the delamination is more difficult to initiate and propagate because of the restraint of the cell components. This design should therefore be able to survive oxidation strains of up to 1% for an anode thickness of 10 μm.

Relationships for calculating the curvature and residual stress for layered composites from the difference in thermal or isothermal expansion are given in [60]. Thermal stresses caused by fixing the cell in the stack or by temperature gradients can be added to this model if known, for example, from finite element simulations.

The use of the relationships is exemplified in Fig. 4, where the radius of curvature is given as a function of the thickness of the reoxidized layer for a particular reoxidation expansion (cell thickness ~0.27 mm). It can be seen that the behaviour (change in direction) as well as the absolute values agree with the experimental data (Fig. 2 [51]). Similar agreement was observed for the thicker specimens. Based on these results, it can be suggested that reoxidation leads to a strain of 0.15% in agreement with the results reported in [59] and a reoxidation strain of 0.75% in the anode, yielding a

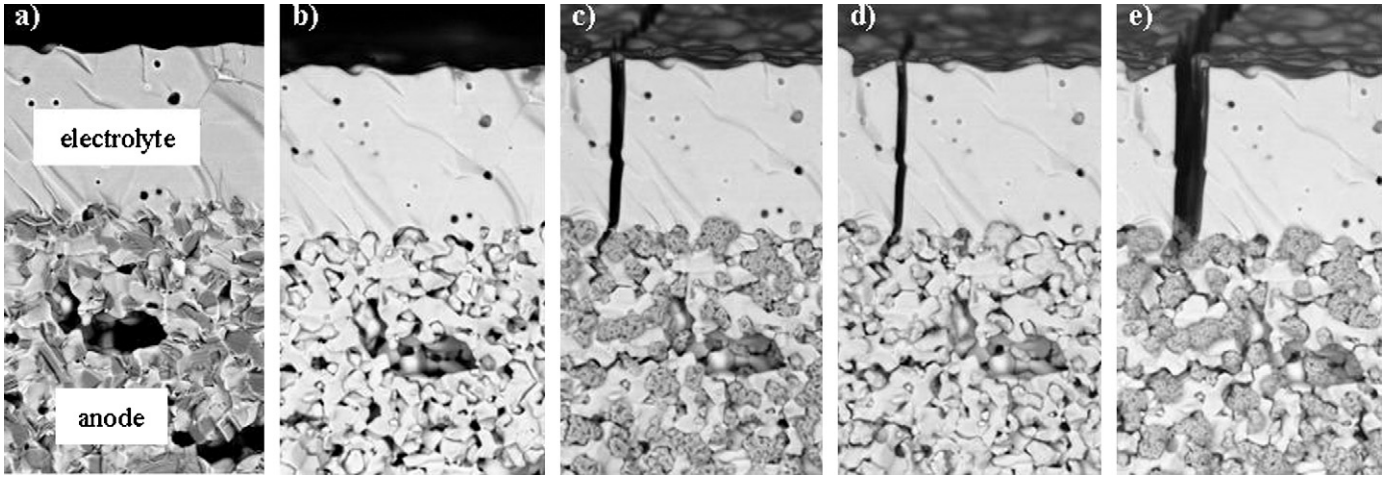

Fig. 3. SEM study on microstructural changes in anode and substrate due to reduction/reoxidation cycles: (a) initial co-fired state, (b) reduced, (c) reoxidized, (d) re-reduced and (e) re-reoxidized.

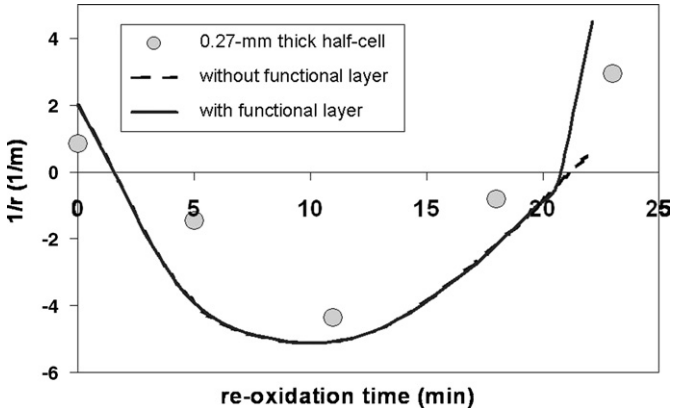

Fig. 4. Curvature as a function of the reoxidized layer thickness.

tensile stress of more than 450 MPa in the electrolyte layer at the end of the reoxidation process. This stress is in the range of the sum of the compressive stress (~200 MPa at 800 °C) and strength of the electrolyte at high temperatures (265 MPa at 900 °C [60]). The large strain in the anode is also reflected in the small cracks visible close to the electrolyte in the anode in Fig. 3. The significance of the anode for the fracture of the electrolyte is supported by observations reported in [3,4].

If sufficient experimental data are available, the analysis can be refined by the statistical variability in the failure, usually represented by the Weibull distribution of the fracture stress values. This was not considered in [51,59,61]. In the case of thin layers like the electrolyte, it has been suggested that a lower limit of the fracture stress – a so-called threshold stress – exists. This would be more appropriate in such an analysis than the characteristic strength [62].

A parametric study of the effect of the substrate, anode and the use of an inert-substrate (reoxidation expansion substrate 0.2%, anode 2%, $\Delta\alpha$-anode-electrolyte $2 \times 10^{-6}\,K^{-1}$, stress-free at 1150 °C, stiffness of electrolyte 200 GPa, substrate and anode 68 GPa [50]) based on the relationships given in [60] revealed that a reduction in the thickness of the anode substrate increases the residual stress in the electrolyte as the substrate carries part of the strain. This is also the case when the substrate does not display any reoxidation strain (inert ceramic); in the latter case a substrate thickness of ~300 μm is sufficient to avoid fracture. In this case as well, the characteristic strength of the electrolyte at 800 °C was used as a fracture criterion. If no substrate exists, either the thickness of the anode layer must be significantly reduced or the thickness of the electrolyte layer must be increased in order to avoid macroscopic fracture. It should be noted that the assumed strains are only estimates and a reduction in the reoxidation expansion of the substrate and the anode layer has the strongest impact on reoxidation stability.

4. Reoxidation of cell- and stack-type structures

For SOFC applications, it is necessary to characterize, on the one hand, the basic mechanisms associated with the reoxidation of Ni, the influence of the reoxidation on the integrity of the substrate and the functional layers on a microscopic scale, and, on the other hand, the influence of the reoxidation parameters such as gas flow rate, temperature and time (operational conditions) on half-cells and stack-like structures, e.g. "half-cassettes". In this context, "half-cell" refers to components based on the substrate coated and end-manufactured with anode and electrolyte but with no cathode layer. "Half-cassette" refers to components consisting of half-cells sealed to a window frame (as part of a repeating unit typically used within a SOFC stack), which are tested in specially designed test equipment. These tests are more complex than cell tests but simpler than stack testing. The main goal in testing sealed half-cells is to characterize the influence of bending constraints and behaviour within a sealed system. Half-cells which can freely bend three-dimensionally during reoxidation can reduce the internal stresses by warping. If the cells are sealed in a frame and mounted in a test stand, the available free moving space is minimized and the stresses can only be diminished by cracking (either within the cell itself or between cell and frame within the sealant). Therefore the "cell response" must differ between free bending and constrained bending. In fact, the sealed bending status of the cell corresponds to that of a cell within a stack, and is thus a more realistic test. Based on this idea, various tests on the influence of the above-mentioned operation-like parameters were carried out to separate the main factors of influence from those that can be neglected, and to compare the macroscopic behaviour of the components during free bending and constrained warpage.

4.1. Half-cells

Half-cells consisting of a thick substrate (thickness between 500 and 1500 μm) based on Ni–8YSZ and coated with an anode (Ni–8YSZ, 7 μm) and an electrolyte (8YSZ, 10 μm), co-fired at 1400 °C for 5 h, were tested inside a glass cylinder mounted in a furnace. The glass recipient was flushed with either ambient

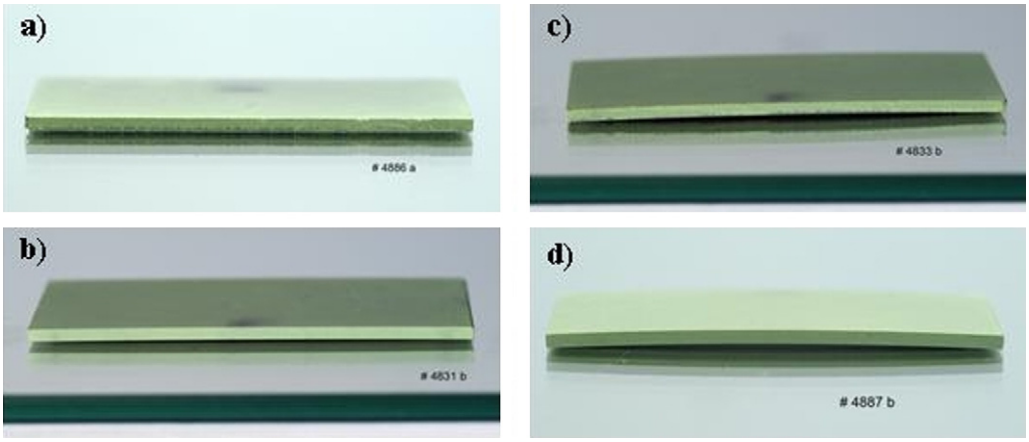

Fig. 5. Warpage of half-cells (substrate thickness 1500 μm) during reoxidation at 800 °C for 15 min with varying air flux; DoOs: (a) 8%, (b) 20%, (c) 28% and (d) 38% (the electrolyte is on the bottom side) [36,39,63].

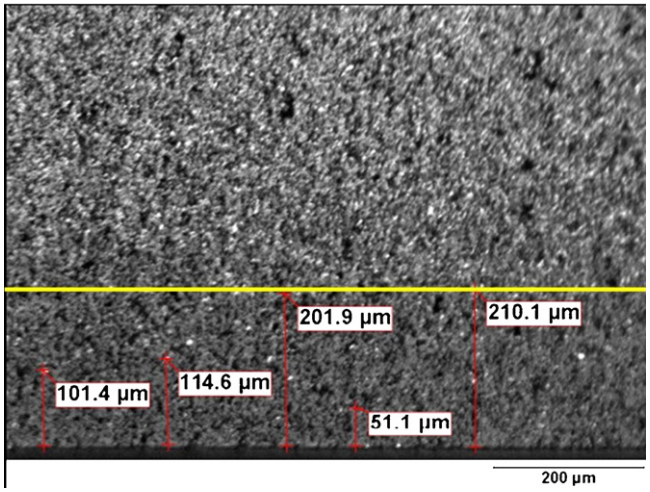

Fig. 6. Optical microscopy of a half-cell reoxidized for 12 h at 800 °C and with a DoO of 25% (on the bottom side, the substrate border is the starting point for the depth measurements of the borderline between oxidized and reduced Ni phase).

air (for reoxidation) or a mixture of 4% hydrogen in argon (for re-reduction). Nitrogen can be flushed between reoxidation and re-reduction cycles as an inert gas agent. The varied reoxidation parameters are: temperature of reoxidation (300–800 °C), time of reoxidation (1 min to 48 h) and air flux (0–1200 mL min^{-1} at 0 °C, 1 atm). When one parameter was changed the other two were kept constant. Fig. 5 shows the variation in half-cell bending during reoxidation of the samples at 800 °C for 15 min with varying degrees of oxidation (DoO; variation parameter was air flux) [36]. Concerning the results presented here, no results from experiments at temperatures below 500 °C were included because there is negligible difference in results obtained at 500, 400 and 300 °C with respect to warping and electrolyte cracking.

From Fig. 5 the following conclusions can be drawn: the higher the DoO, the stronger the concave bending of the cells. Even at only 8% reoxidation, the outer side of the substrate is completely oxidized (green colour). No cracks are visible up to 38% reoxidation. The anode is still in a reduced (grey colour) state (not shown in figure). If such samples are cut, polished and characterized by optical microscopy, a borderline is visible between the reoxidized outer part and the remaining reduced state at the inner part.

Fig. 6 shows, as an example, a half-cell reoxidized at 800 °C for 12 h and with a DoO of 25%. The end of the five red lines drawn from the substrate surface indicates the points of investigation with the SEM. At these points the substrate was analyzed to determine whether Ni or NiO was the dominant phase. The labels state the distance to the substrate surface. From these investigations a borderline (yellow line) at about 200 µm from the surface of the substrate defining the reoxidized part of the substrate could be determined. In this region NiO is the dominant phase, although some remaining metallic Ni particles can be seen in the reoxidized region. This relatively sharp border between the oxidized and reduced Ni is only visible when the samples are oxidized at higher temperatures. Comparing equivalent reoxidation parameters on the same samples by only varying the reoxidation temperature from 800 to 600 °C reveals a completely different substrate microstructure with respect to reoxidation homogeneity. Fig. 7 shows optical microscopy micrographs of half-cells reoxidized at 600 or 800 °C with the same DoO (41%). It is obvious that for the sample reoxidized at 600 °C there is no border between an oxidized and a reduced metal region within the cermet. The whole substrate is reoxidized homogeneously from the substrate surface up to the anode [39]. The reason for the grey colour of the substrate is that only the surface of the nickel particles is oxidized (see the following sections).

One effect of the varying homogeneity of reoxidation is that the bending behaviour changes. Samples reoxidized at higher temperatures show more bending than samples reoxidized at lower temperatures. There is a clear correlation between homogeneity of the reoxidation and bending of the half-cells. Consequently, samples reoxidized at lower temperatures can withstand higher DoOs with respect to electrolyte cracking due to better oxidation homogeneity and less porous reoxidation of the metallic nickel. Therefore another consequence of better homogeneity is superior reoxidation tolerance. This means that the higher the homogeneity of the reoxidation, the higher the tolerable DoO, the smaller the bending and the better the cell with respect to redox tolerance.

When the microstructure of samples reoxidized completely is compared to those reoxidized only to a limited degree at 700 °C, it can be seen that the sample reoxidized to a limited degree shows a core–shell structure for the Ni particles. The outside of the Ni particles is oxidized, while the core is still in a metallic state (Fig. 8).

A comparison of specimens reoxidized at 600 or 800 °C shows the difference in DoO and electrolyte cracking. While samples oxidized at 800 °C can reach DoOs of up to 74%, even with high air flux and under comparable conditions, samples aged at 600 °C can only be oxidized to 51%. In addition, the samples oxidized at 800 °C already show electrolyte cracking at a DoO of 25%, while those samples oxidized at 600 °C show no cracking even at a DoO of 51% (Fig. 9).

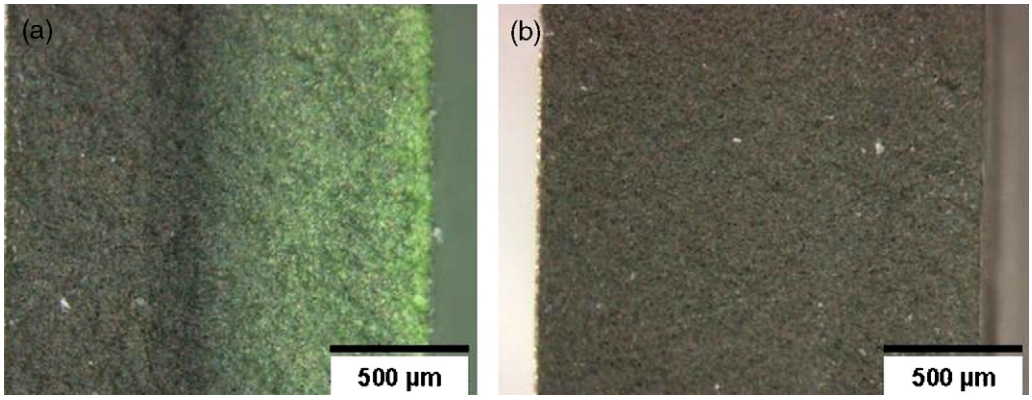

Fig. 7. Optical microscopy images of two samples reoxidized at (a) 800 °C and (b) 600 °C; warm-pressed anode substrate with a thickness of 1.5 mm, anode layer with a thickness of 7 µm, electrolyte with a thickness of 10 µm [39].

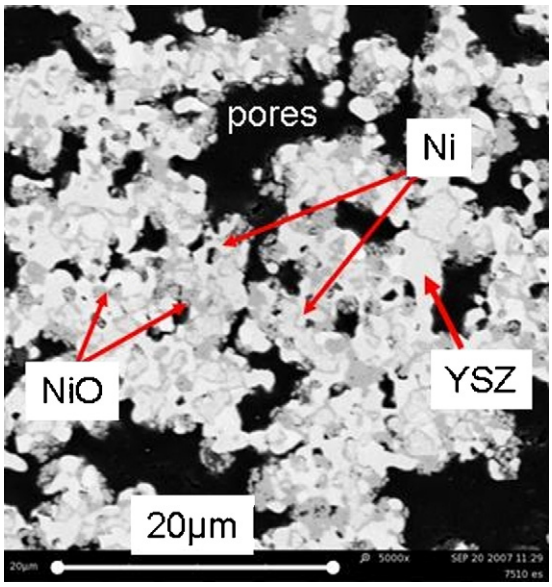

Fig. 8. SEM micrograph of a sample with a DoO of 39% reoxidized at 700 °C; core–shell structure of partly reoxidized nickel.

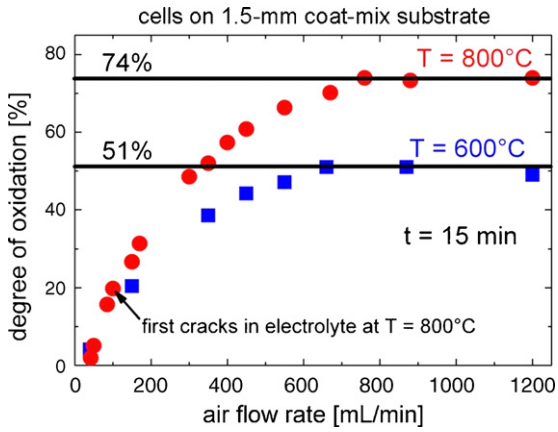

Fig. 9. Comparison of DoOs of samples oxidized at 800 °C (dots) and 600 °C (squares) depending on the air flow rate (at 0 °C, 1 atm).

Based on these findings, a mechanism for the deterioration of half-cells is proposed (reoxidation at temperatures ≥700 °C):

- Partially oxidized state (reoxidation front below neutral axis) (Fig. 10):
  - parts of the substrate are elongated during oxidation;
  - electrolyte remains under compressive stresses;
  - if reoxidation front does not pass the neutral axis, the bending direction remains concave with respect to the substrate;
  - electrolyte should not crack;

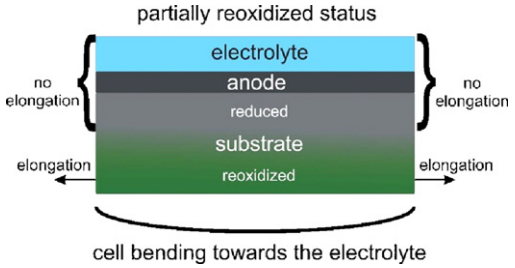

Fig. 10. Scheme of half-cell in partially reoxidized state at $T \geq 700$ °C.

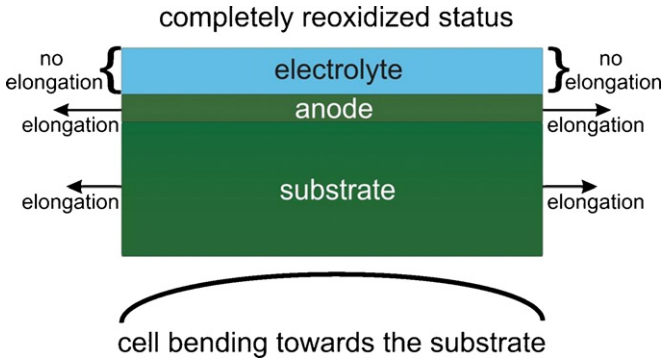

Fig. 11. Scheme of half-cell in completely reoxidized state at $T \geq 700$ °C.

  - radius of warpage depends on DoO and homogeneity of oxidation.

At these high reoxidation temperatures, there is a gradual change from the partly oxidized to the completely oxidized state.

- Completely oxidized state (Fig. 11):
  - substrate and anode are elongated;
  - warpage changes from concave to convex;
  - electrolyte comes under tensile stresses;
  - electrolyte cracks.

Additionally, another status can be proposed (mostly occurring at temperatures <700 °C) (Fig. 12):

- homogeneous distribution of Ni and NiO within the substrate;
- no gradient of the degree of oxidation;
- cell bending only slightly towards the electrolyte (concave).

Another important factor for the reoxidation behaviour of cells is the substrate thickness and porosity. By reducing the substrate thickness from 1500 to 1000 µm (retaining the manufacturing technique and substrate microstructure), it was possible to enhance the redox stability of half-cells. Half-cells based on the 1000-µm substrates can be oxidized to higher DoOs without electrolyte cracking. Tests at 600 °C showed that samples with 1500-µm substrates can be reoxidized to DoOs of 60% without electrolyte cracking, while those cells with 1000-µm substrates can be reoxidized completely (100%) without the electrolyte cracking. For these thinner substrates, the fixed microstructure (Ni–YSZ ratio, porosity) ensures more homogeneous oxidation for given reoxidation parameters and therefore reduced bending and thus initial electrolyte cracking at higher DoOs. Additionally, the ability of the substrate to bend the half-

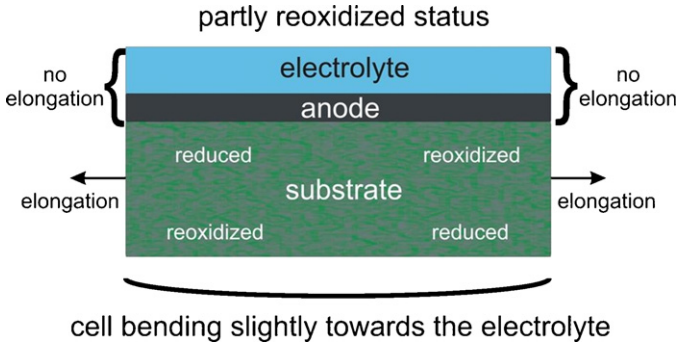

Fig. 12. Scheme of half-cell in party reoxidized state at $T < 700$ °C.

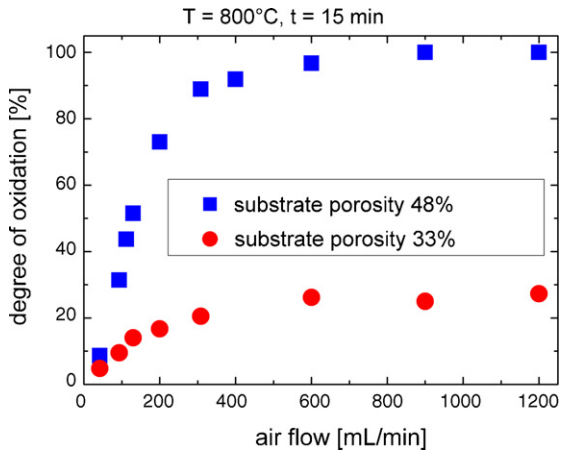

Fig. 13. Comparison of porous and more dense tape-cast anode-substrate half-cells; DoO depending on the air flow rate (0 °C, 1 atm) at a given time and temperature, electrolyte cracking for both types of samples at DoOs ≥ 20%.

cell is reduced due to a higher ratio of electrolyte to substrate thickness. However, reducing the substrate thickness even further does not result in a further improvement of redox stability [39].

Tests carried out at half-cells based on thinner substrates (500 μm) produced by tape casting and with a lower porosity (33 vol.%) showed better reoxidation tolerance than those with a higher substrate porosity (48 vol.%). A comparison of two thin substrates with different porosity showed that the more porous substrate at 800 °C with an air flux of 0.2 nL min^{-1} for 15 min can be oxidized to about 75% with cracks in the electrolyte. The samples based on substrates with reduced porosity reoxidized under the same conditions show DoOs of less than 20% and therefore no electrolyte cracking (see Fig. 13).

It is thus concluded that lower substrate porosity enhances cell tolerance with respect to redox cycling because gas transport into the pore structure is the rate-determining process. Single-cell testing (50 mm × 50 mm) of comparable cells based on tape-cast substrates show the first restriction on anodic diffusion at fuel utilizations of more than 55%. The balance between cell power output and cell redox tolerance must therefore be optimized as the two parameters are in competition.

4.2. Half-cassettes

For the tests with so-called half-cassettes, half-cells of the above-mentioned specifications and with dimensions of approx. 150 mm × 80 mm (or 100 mm × 100 mm) were sealed with a glass-ceramic (or a metal) in a Crofer22APU window frame (thickness 500 μm). These half-cassettes were mounted in test equipment specially designed and sealed to the surrounding sample holder with Thermiculite XJ866 (mica). The test equipment was placed into a glass cylinder and the substrate side of the half-cell was flushed with ambient air (for oxidation), argon/4% hydrogen (for reduction) and, if necessary, nitrogen as a flushing gas between oxidation and reduction. For the tests, the same conditions were set as for the free-standing half-cells (only a change in the flux is necessary as the air flux must be adapted to the greater substrate area and therefore the higher amount of Ni in the samples).

A schematic overview of the test equipment is given in Fig. 14. Fig. 15 shows a picture of the test equipment.

A typical result from a test run at 600 °C is shown in Fig. 16. The DoO is approx. 3% and therefore most of the substrate is still in a reduced state (grey colour). Only a rim is visible at the gas inlet side and the two bypass sides. In addition, a coloured structure can also be seen at the end of the partially oxidized zone. This is due to the gas distribution channels in the test setup. Enhancing the DoO from 3 to 10% does not change the visible result. Only the colour within the oxidized regions becomes greener (see Fig. 17).

When the temperature is raised from 600 to 800 °C, the border between the reoxidized and reduced regions becomes clearly visible (Fig. 18), implying that the reoxidation is more inhomogeneous. As a consequence of the reduced reoxidation homogeneity, specimens reoxidized at 800 °C to DoOs of 10% were cracked macroscopically. Cracking normally starts at the air-in edge of the samples and at the sample side edges (as can be seen in Fig. 18).

Based on the results obtained, it can be concluded that half-cells of the same type can only withstand reoxidation under sealed conditions to much lower DoOs than in the case of free half-cells. While unsealed half-cells can be reoxidized to approx. 20–25% at 800 °C without electrolyte cracking, the samples in a sealed state already

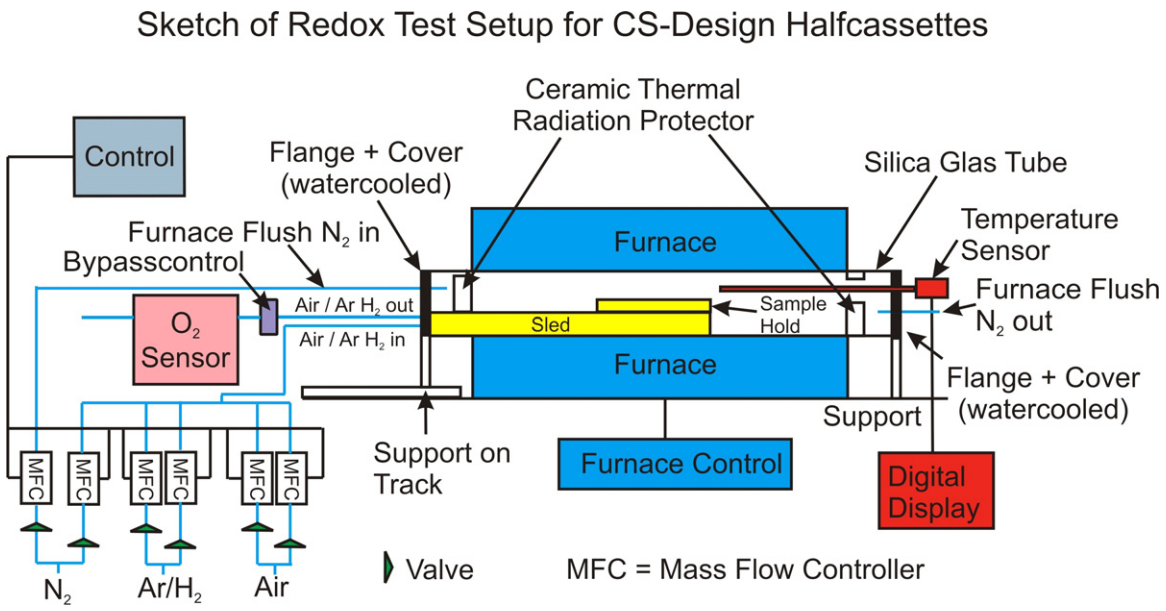

Fig. 14. Test setup for redox testing of half-cassettes (schematic).

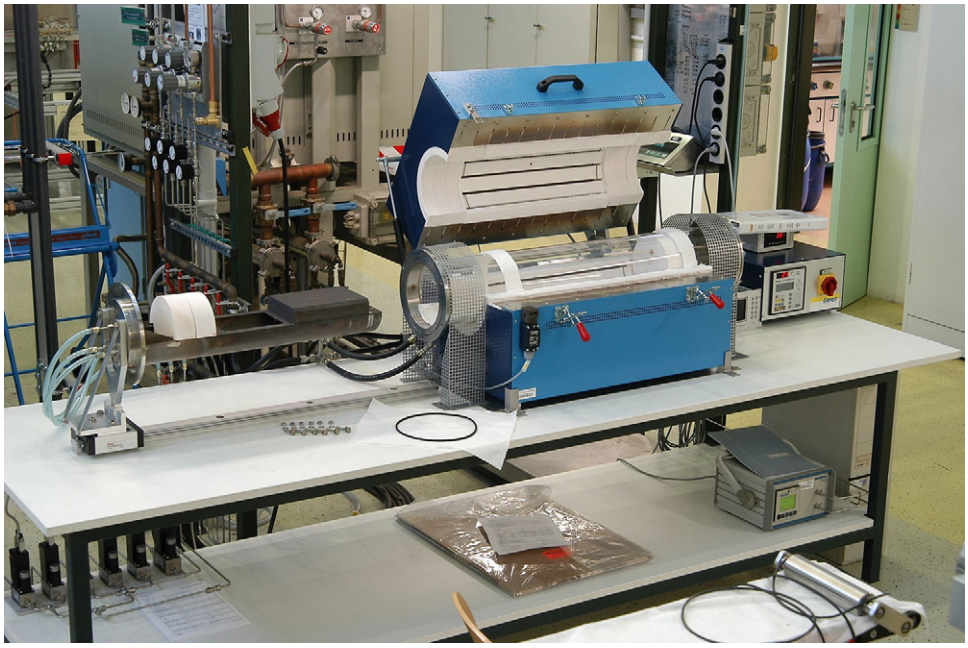

Fig. 15. Test setup for half-cassette redox testing.

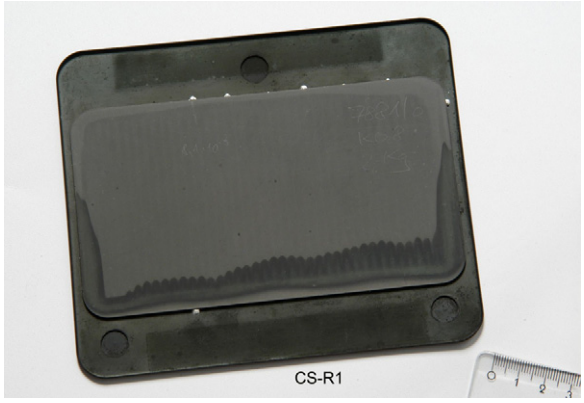

Fig. 16. Photograph of a half-cassette reoxidized at 600 °C to a DoO of 3%; view of the substrate.

fail at DoOs of ~10% by either electrolyte or complete cell cracking. This must be taken into consideration when transferring results from free-standing cell tests to nearly operational conditions. Cell cracking in the sealed state begins earlier due to:

- minimized or constrained elongation at the *x*–*y* level and/or
- constrained cell warping and/or
- inhomogeneous reoxidation; in addition to the tests carried out on free-standing samples, which reveal inhomogeneities in the *z* direction (over the substrate thickness), there is an additional inhomogeneity in the *x*–*y* direction; thus inhomogeneities are formed in all spatial directions

It is still unclear what factor plays the key role and to what extent each factor contributes to the minimized reoxidation stability. It can only be said that the failure of the cell in a sealed status is a sum effect of the above-mentioned reasons.

Sealing the air flow edges of the cells or closing the bypass did not change the shape of the reoxidation profile on the samples significantly. Therefore, complex and expensive edge sealing arrangements can be abolished.

Initial stack testing under conditions comparable to the tests on half-cassettes shows similar results. The OCV and power output remain constant during redox cycling to DoOs of less than 1.5%. It can therefore be concluded that no cracking occurs.

Fig. 17. Photograph of a half-cassette reoxidized at 600 °C and with a DoO of 10%; view of the substrate.

Fig. 18. Photograph of a half-cassette reoxidized at 800 °C to a DoO of 10%; view of the substrate, red ellipses highlight the macroscopic cracks.

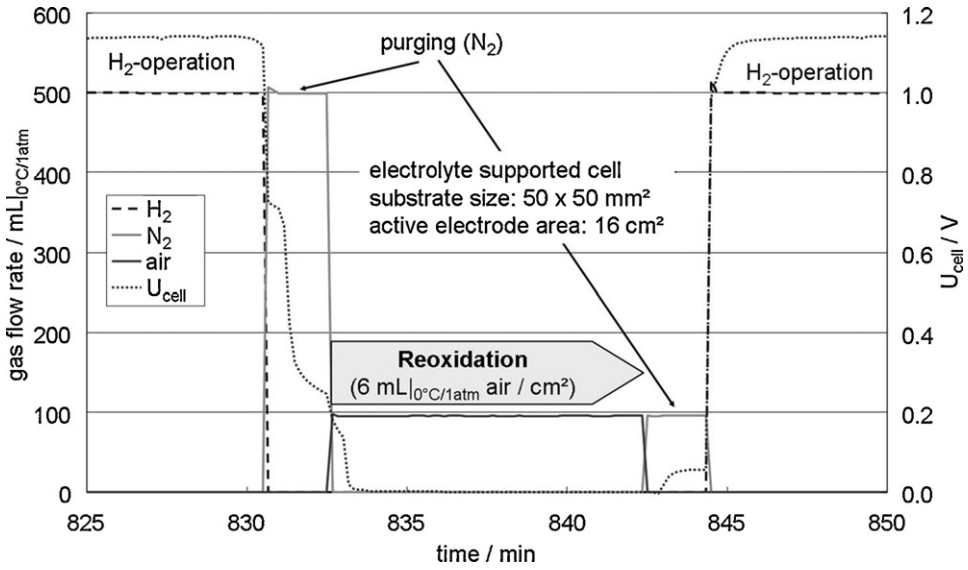

Fig. 19. Time flow of a 10-min reoxidation cycle: after purging the anode gas compartment with nitrogen, a well-defined flow of air (6 mL air cm^{-2} active electrode area) was fed to the anode for 10 min. After this, the anode gas compartment was purged with nitrogen at a similar flow rate. To re-reduce the anode after this reoxidation procedure, fuel (H_2) was provided to the anode again.

5. Redox-induced electrochemical degradation of single cells

In addition to mechanical failures resulting in the electrolyte cracking in anode-supported cells (ASCs) or the anode delaminating in electrolyte-supported cells (ESCs), a temporal reoxidation and subsequent re-reduction within the anode functional layer leads to microstructural changes that result in an increase of the anode polarization resistance.

To study the impact of reoxidation cycles on the electrochemical performance of anode- and electrolyte-supported cells, single cells with a Ni-based cermet anode exhibiting an active electrode area of 16 cm^2 were tested in a single-cell test bench as described in [64].

The redox stability of different types of electrolyte- and anode-supported cells was analyzed at an operating temperature of 800 °C. In Table 1 information about the cells and especially the anodes is given.

Each cell was subjected to 50 short redox cycles (reoxidation time: 1 min) and subsequently 50 long redox cycles (reoxidation time: 10 min). In Fig. 19, the time flow of a 10-min reoxidation cycle is displayed.

To determine the decrease in performance induced by the redox cycles, a CV characteristic was measured every 10 cycles. In Fig. 20, the normalized power density $p_{0.7V}(n)$[1]$/p_{0.7V}(0)$ and OCV after 50 short redox cycles and additional 50 long redox cycles is illustrated for different types of electrolyte- and anode-supported cells.

Whereas the OCV of electrolyte-supported cells is not affected by redox cycling, the anode-supported cells showed a notable decrease and even complete failure (ESC type II) after 50 short cycles. This can be attributed to the formation of cracks in the electrolyte. In case of a reoxidation time of 10 min, the OCV of all anode-supported cells dropped to zero after less than 5 cycles.

All electrolyte- and anode-supported cells investigated in this study showed a decrease in power density after 100 redox cycles. This is related to microstructural changes resulting in an increased ASR and, in the case of anode-supported cells, the formation of (micro-)cracks in the electrolyte. The degree of degradation depends on the cell type and the reoxidation duration. It should be noted that in some cases (e.g. ESC type 3) an increase in performance was observed during the first redox cycles. One reason for the different degradation behaviour of electrolyte-supported cells has to be attributed to the anode composition. In case of Ni/Y_2O_3 doped ZrO_2–cermets redox cycling leads to Ni-agglomeration resulting in a loss of three phase boundaries and electronic contact between the Ni particles. In Ni/Gd_2O_3 doped CeO_2 anodes the mixed ionic electronic conductivity and catalytic activity of ceria lowers these degradation effects. Nevertheless a strong degradation of these anodes during redox cycling is obvious.

To study the impact of the reoxidation temperature on the evaluation of cracks in the electrolyte, as well as on the decrease in cell performance, ASC type 1, an anode-supported cell with a 1-mm Ni/8YSZ substrate as already described in the previous section, was redox-cycled at 600, 700 and 800 °C using the same procedure (50 short redox cycles + 50 long redox cycles). The relative change in power density is shown in Fig. 21.

It is obvious that a decrease in the operating and reoxidation temperature results in a decreased degradation in performance.

Considering the decrease in OCV (Fig. 22), three different causes for the decrease in performance are obvious:

1. At constant OCV (no formation of microcracks) a partial reoxidation of the anode functional layer, resulting in microstructural changes and Ni-agglomeration, leads to a decrease in power density (cycle 1–50 at 700 °C).
2. Even a small decrease in OCV caused by the formation and growth of microcracks (cycle 30–50 at 800 °C/cycle 51–100 at 700 °C) results in an enhanced decrease in power density.

Table 1
Electrolyte- and anode supported cells tested with respect to redox-induced electrochemical degradation.

Cell	Manufacturer	Anode material	Anode thickness[a]
ESC type 1	IWE [65]	Ni/8YSZ	30. . .50 μm
ESC type 2	A	Ni/Gd_2O_3 doped CeO_2	~40 μm
ESC type 3	B	Ni/Gd_2O_3 doped CeO_2	~30 μm
ASC type 1[b]	FZJ [39]	Ni/8YSZ	~1000 μm
ASC type 2	C	Ni/YSZ	~400 μm
ASC type 3	A	Ni/YSZ	~500 μm

[a] In case of ASCs: thickness of anode functional layer + thickness of anode substrate.
[b] Referred to earlier as cells with 1000-μm substrates.

[1] Power density at a cell voltage of 0.7 V after n reoxidation cycles.

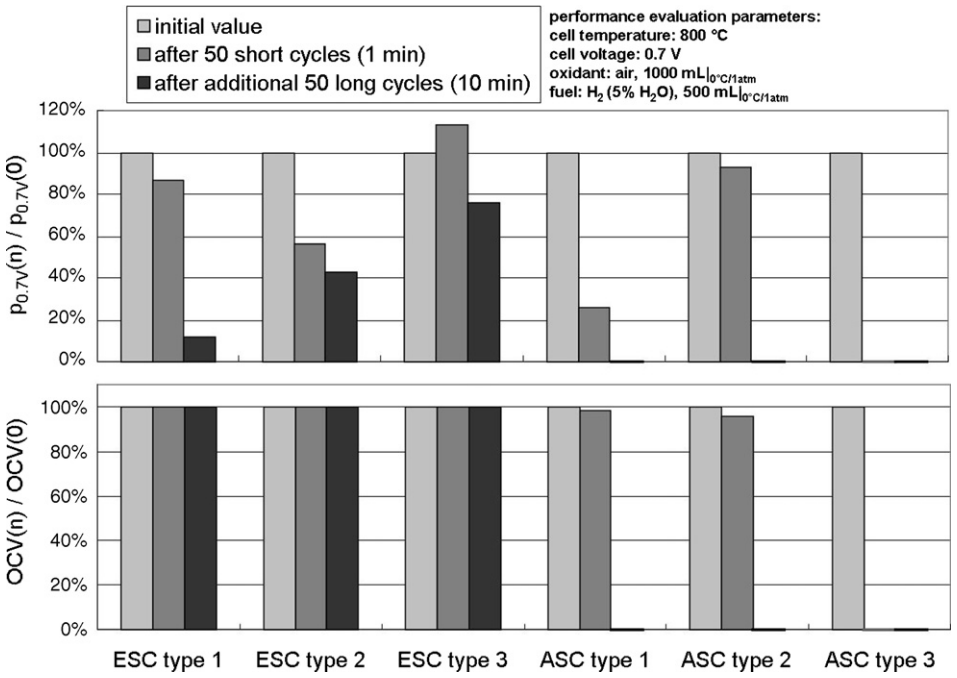

Fig. 20. Normalized power density and OCV of different types of electrolyte- and anode-supported cells during redox cycling at 800 °C.

3. Next to these "real" degradation processes, warpage of the single cell (see Section 4.1) results in similar behaviour. Deterioration of the sealing can result in a decrease in OCV, and a (reversible) loss in power density could occur due to a contact loss between the electrode and the current collector. We assume that these effects are the reason for the fluctuating power density at 600 °C. The severe decrease in power density (48%) observed between cycles 50 and 60 is related to warpage of the cell during the first reoxidation over a period of 10 min. Due to the slow reduction of the cermet at temperatures below 650 °C [26], only an incomplete re-reduction is achieved within the re-reduction time of 8 min. Therefore an insufficient contact results in performance loss during the following CV measurements.

In Fig. 23, the degradation of type 1 anode-supported cells is shown for different reoxidation times and air flow rates corresponding to an O_2 amount of 3 and 6% oxidation of Ni in the anode. The results show that for rather short reoxidation times (~1 min), the degradation is only affected by the reoxidation time. The overall amount of oxygen introduced to the anode does not cause any degradation as long as the reoxidation time is sufficiently short.

The electrochemical tests during redox cycling show that redox cycles that do not affect the mechanical integrity of the cell may nevertheless cause severe performance degradation. Partial reoxidation within the anode functional layer causes microstructural changes that generally lead to an increased polarization resistance.

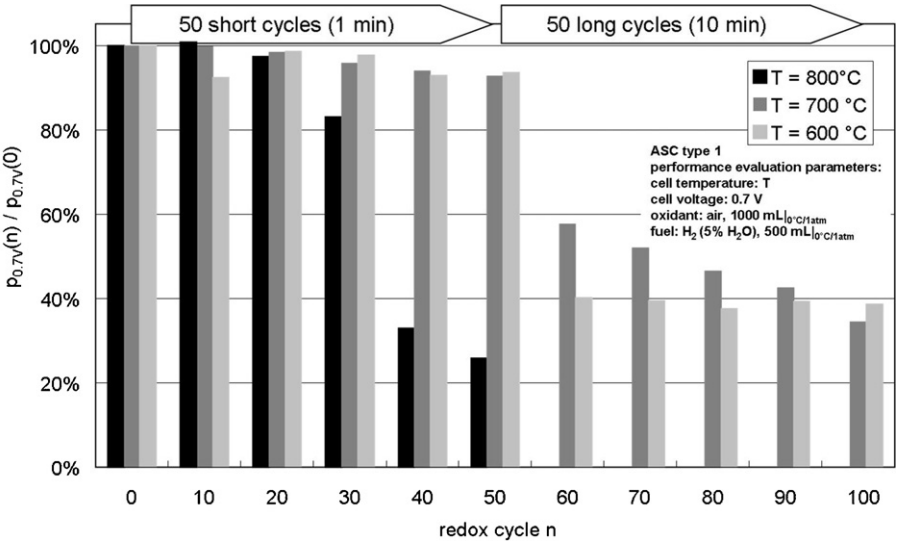

Fig. 21. Normalized power density of ASC type 1 during redox cycling at 800, 700 and 600 °C.

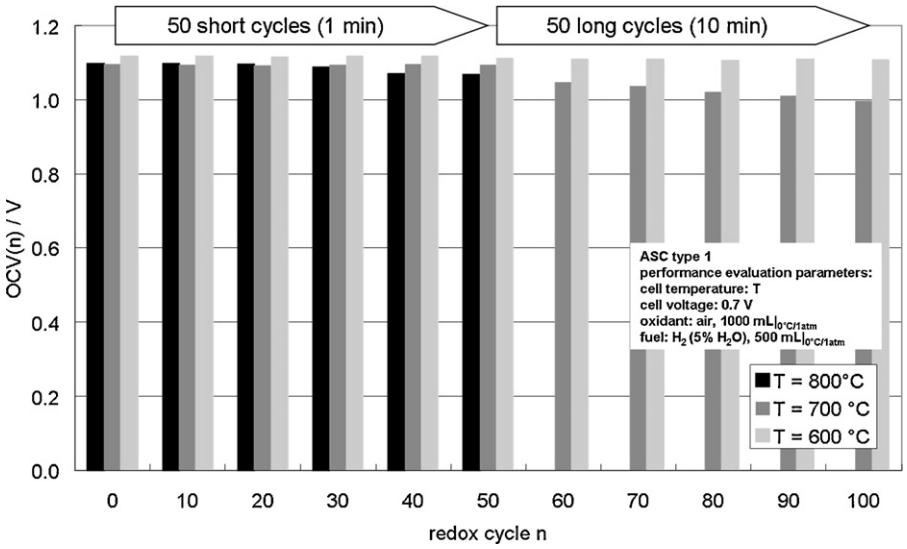

Fig. 22. OCV of ASC type 1 during redox cycling at 800, 700 and 600 °C.

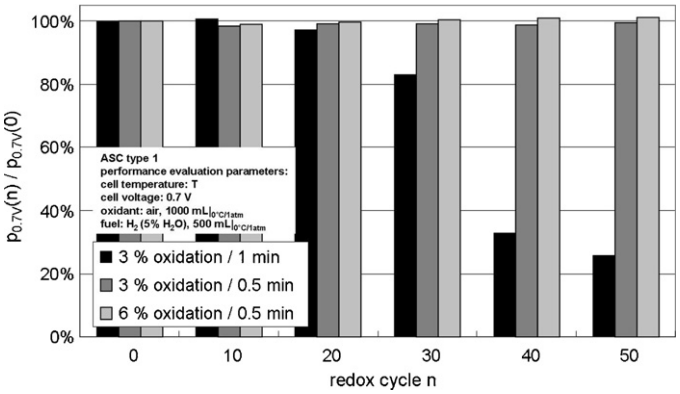

Fig. 23. Normalized power density of ASC type 1 during redox cycling under different conditions. Three and 6% oxidation corresponds to an oxygen amount required to reoxidize 3 and 6% of the overall Ni amount in the anode.

6. Conclusions: reoxidation of anode-supported SOFCs

Metallic nickel in the substrate and anode in anode-supported SOFCs reoxidizes when air enters the fuel cell either intentionally or unintentionally at high temperatures and leads to a sponge-like NiO structure that occupies more volume than in the original oxidized (as-prepared) state. This volume expansion causes stresses within the substrate, the anode and the electrolyte. If the stresses exceed the strength of the electrolyte, cracks form and the cell fails catastrophically. The characterization of simple Ni and YSZ pellets and of free-standing half-cells (cells without cathode layers) show an acceptable redox behaviour. Reoxidation of 20–25% (at 800 °C) and even higher values at lower temperatures seem to be tolerable without electrolyte cracking. The major factors affecting reoxidation stability appear to be: (a) the degree of reoxidation, (b) the homogeneity of reoxidation, and (c) the temperature at which reoxidation occurs.

The characterization of half-cassettes (half-cells sealed to metal frames) with respect to redox stability shows that reoxidation becomes more problematic in an operation-like environment. In such configurations, anode-supported cells are able to withstand redox cycles with drastically reduced DoOs in the region of around 10% for a few cycles and around 1% for many cycles. By redox cycling of stacks with maximum DoOs of about 1.5%, this was confirmed for a limited number of cycles. However, cell and stack testing with respect to redox cycling needs further investigation. Special limiting factors for the redox tolerance and stability of cells in operation-like environment appear to be: (a) the fixed position of the cell allowing only limited expansion and deflection, and (b) the inhomogeneous reoxidation in all three spatial directions due to the incident flow via one edge of the cell. Hence, reoxidation induces high stresses in the cell frame assembly, causing the electrolyte or even the cell to crack or leading to disruption of the sealing between cell and metal frame. In single-cell tests, it was also be shown that redox cycling, which does not affect the mechanical integrity of the cell, can nevertheless cause severe cell degradation.

Based on these observations, it can be concluded that intentional air break-in at the anode side of SOFCs should be avoided. This also applies to electrolyte-supported cells. Hence, system solutions such as bypass tubes, oxygen getters and flushing with inert gases cannot be totally neglected and should be considered if affordable and acceptable with respect to the mass and complexity of the system. If ingress of air cannot be avoided due to technical limitations, the amount of air should be strongly restricted and the exposure time of the anode side surface should be strictly limited to reduce the amount of air diffusing into the substrate and the anode and thus reoxidizing the nickel to minimize the degree of oxidation. Coating Ni with reactive elements such as Y, Zr, La and Ce or their oxides reduces the oxidation rate and changes the morphology of the oxide surface by changing the scale growth from primarily outward to primarily inward [66]. Such coatings therefore have the potential to further reduce the degree of oxidation of the substrate after an intended redox cycle. However, a suitable coating technology for coating the outer surface of the anode as well as its inner structure has to be found and established.

The redox tolerance of both cell types, anode- and electrolyte-supported cells, is strongly limited. Unintentional reoxidation will lead to system failure, as the amount of oxygen breaking in as well as the oxidation conditions (time and temperature) cannot be controlled.

Acknowledgement

The authors gratefully acknowledge the financial support from various Federal Ministry of Economics (BMWi) projects.

References

[1] D. Sarantaridis, A. Atkinson, Fuel Cells 7 (2007) 246–258.

[2] T. Klemensø, C.C. Appel, M. Mogensen, Solid-State Lett. 9 (2006) A403–A407.
[3] T. Klemensø, C. Chung, P.H. Larsen, M. Mogensen, J. Electrochem. Soc. 152 (2005) A2186–A2192.
[4] D. Waldbillig, A. Wood, D.G. Ivey, Solid-State Ionics 176 (2005) 847–859.
[5] D. Waldbillig, A. Wood, D.G. Ivey, J. Power Sources 145 (2005) 206–215.
[6] J. Malzbender, E. Wessel, R.W. Steinbrech, L. Singheiser, Solid-State Ionics 176 (2005) 2201–2203.
[7] Y. Zhang, B. Liu, B. Tu, Y. Dong, M. Cheng, Solid-State Ionics 176 (2005) 2193–2199.
[8] D. Fouquet, A.C. Müller, A. Weber, E. Ivers-Tiffée, Ionics 9 (2003) 103–108.
[9] A. Wood, M. Pastula, D. Waldbillig, D.G. Ivey, J. Electrochem. Soc. 153 (2006) A1929–A1934.
[10] M. Pihlatie, A. Kaiser, P.H. Larsen, M. Mogensen, J. Electrochem. Soc. 156 (2009) B322–B329.
[11] L. Blum, H.-P. Buchkremer, S. Gross, A. Gubner, L.G.J. (Bert) de Haart, H. Nabielek, W.J. Quadakkers, U. Reisgen, M.J. Smith, R. Steinberger-Wilckens, R.W. Steinbrech, F. Tietz, I.C. Vinke, Fuel Cells 7 (2007) 204–210.
[12] J. Larminie, A. Dicks, Fuel Cell Systems Explained, second ed., Wiley, 2003.
[13] M. Radovic, E. Lara-Curzio, Acta Mater. 52 (2004) 5747–5756.
[14] J.T. Richardson, R. Scates, M.V. Twigg, Appl. Catal. A 246 (2003) 137–150.
[15] T.A. Utigard, M. Wu, G. Plascencia, T. Marin, Chem. Eng. Sci. 60 (2005) 2061–2068.
[16] A. Atkinson, Philos. Mag. B 55 (1987) 637–650.
[17] A. Atkinson, Rev. Mod. Phys. 57 (1985) 437–470.
[18] A. Atkinson, R.I. Taylor, A.E. Hughes, Philos. Mag. A 45 (1982) 823–833.
[19] A. Atkinson, R.I. Taylor, P.D. Goode, Oxid. Met. 13 (1979) 519–543.
[20] A. Atkinson, R.I. Taylor, Philos. Mag. A 39 (1979) 581–595.
[21] A. Atkinson, D.W. Smart, J. Electrochem. Soc. 135 (1988) 2886–2893.
[22] R. Karmhag, G.A. Niklasson, M. Nygren, J. Mater. Res. 14 (1999) 3051–3058.
[23] R. Karmhag, G.A. Niklasson, M. Nygren, J. Appl. Phys. 85 (1999) 1186–1191.
[24] N.M. Tikekar, T.J. Armstrong, A.V. Virkar, J. Electrochem. Soc. 153 (2006) A654–A663.
[25] G. Stathis, D. Simwonis, F. Tietz, A. Moropoulou, A. Naoumides, J. Mater. Res. 17 (2002) 951–958.
[26] S. Modena, S. Ceschini, A. Tomasi, D. Montinaro, V.M. Sglavo, J. Fuel Cell Sci. Tech. 3 (2006) 487–491.
[27] A.C. Mueller, D. Herbstritt, A. Weber, E. Ivers-Tiffée, in: J.A. McEvoy (Ed.), Proceedings of the 4th European SOFC Forum, Lucerne, Switzerland, 2000, pp. 579–588.
[28] M. Cassidy, G. Lindsay, K. Kendall, J. Power Sources 61 (1996) 189–192.
[29] T. Klemensø, M. Mogensen, J. Am. Ceram. Soc. 90 (2007) 3582–3588.
[30] D. Fouquet, A.C. Mueller, A. Weber, E. Ivers-Tiffée, in: J. Huijsmans (Ed.), Proceedings of the 5th European SOFC Forum, Lucerne, Switzerland, 2002, pp. 467–474.
[31] M. Pihlatie, T. Ramos, A. Kaiser, J. Power Sources 193 (2009) 322–330.
[32] M. Pihlatie, A. Kaiser, M. Mogensen, J. Eur. Ceram. Soc. 29 (2009) 1657–1664.
[33] G. Robert, A. Kaiser, E. Batawi, in: M. Mogensen (Ed.), Proceedings of the 6th European SOFC Forum, Lucerne, Switzerland, 2004, pp. 193–199.
[34] L. Grahl-Madsen, P.H. Larsen, N. Bonanos, J. Engell, S. Linderoth, in: J. Huijsmans (Ed.), Proceedings of the 5th European SOFC Forum, Lucerne, Switzerland, 2002, pp. 82–89.
[35] W. Li, K. Hasinska, M. Seabaugh, S. Swartz, J. Lannutti, J. Power Sources 138 (2004) 145–155.
[36] M. Ettler, G. Blaß, N.H. Menzler, Fuel Cells 7 (2007) 349–355.
[37] G. Robert, A. Kaiser, K. Honegger, E. Batawi, in: J. Huijsmans (Ed.), Proceedings of the 5th European SOFC Forum, Lucerne, Switzerland, 2002, pp. 116–122.
[38] J. Malzbender, E. Wessel, R.W. Steinbrech, L. Singheiser, in: E. Lara-Curzio, M.J. Readey (Eds.), Proceedings of the 28th International Conference on Advanced Ceramics and Composites: A, Cocoa Beach, USA, 2005, pp. 387–392.
[39] M. Ettler, N.H. Menzler, H.P. Buchkremer, D. Stöver, in: P. Singh, N.P. Bansal (Eds.), Advances in Solid Oxide Fuel Cells IV: Ceramic Engineering and Science Proceedings, vol. 29, 2008, pp. 33–44.
[40] M. Ettler, Einfluss von Reoxidationszyklen auf die Betriebsfestigkeit von anodengestützten Festoxid-Brennstoffzellen, Schriften des Forschungszentrums Jülich, Reihe Energie & Umwelt/Energy & Environment, Band/Volume 36 (Diss., Bochum, Univ., 2008) (only available in German).
[41] A. Faes, A. Nakajo, A. Hessler-Wyser, D. Dubois, A. Brisse, S. Modena, J. Van Herle, J. Power Sources 193 (2009) 55–64.
[42] D. Waldbillig, A. Wood, D.G. Ivey, in: S.C. Singhal, J. Mizusaki (Eds.), Proceedings of the IXth Int. Conf. on Solid Oxide Fuel Cells, Quebec City, Canada, 2005, pp. 1244–1256.
[43] P. Holtappels, T. Graule, B. Gut, U. Vogt, L.J. Gauckler, M. Jorger, D. Perednis, K. Honegger, G. Robert, S. Rambert, A.J. McEvoy, in: S.C. Singhal, M. Dokiya (Eds.), Proceedings of the VIIIth Int. Conf. on Solid Oxide Fuel Cells, Paris, France, 2003, pp. 1003–1010.
[44] D. Simwonis, G. Stathis, F. Tietz, R.W. Steinbrech, A. Naoumides, in: P. Stevens (Ed.), Proceedings of the 3rd European SOFC Forum, Nantes, France, 1998, pp. 219–228.
[45] A. Mohammadi, J. Pusz, A.L. Smirnova, N.M. Sammes, ECS Trans. 7 (2007) 1409–1418.
[46] D. Sarantaridis, R.A. Rudkin, A. Atkinson, ECS Trans. 7 (2007) 1491–1499.
[47] J. Laurencin, G. Delette, B. Morel, F. Lefebvre-Joud, M. Dupeux, J. Power Sources 192 (2009) 344–352.
[48] Y. Xie, X. Zhang, M. Robertson, R. Maric, D. Ghosh, J. Power Sources 162 (2006) 436.
[49] T. Klemensø, C. Chung, P.H. Larsen, M. Mogensen, in: S.C. Singhal, J. Mizusaki (Eds.), Proceedings of the IXth Int. Conf. on Solid Oxide Fuel Cells, Quebec City, Canada, 2005, pp. 1226–1234.
[50] EU Project SOFC600, Project Reference: 20089.
[51] J. Malzbender, E. Wessel, R.W. Steinbrech, L. Singheiser, Ceram. Eng. Sci. Proc. 25 (2004) 387–392.
[52] J. Malzbender, R.W. Steinbrech, L. Singheiser, Ceram. Eng. Sci. Proc. 26 (2005) 293–297.
[53] W. Fischer, J. Malzbender, G. Blass, R.W. Steinbrech, J. Power Sources 150 (2005) 73–77.
[54] H. Yakabe, Y. Baba, T. Sakurai, Y. Yoshitaka, J. Power Sources 135 (2004) 9–16.
[55] H. Sumi, K. Ukai, M. Yokoyama, Y. Mizutani, Y. Doi, S. Machiya, Y. Akinwa, K. Tanaka, Trans. ASME 3 (2006) 68–74.
[56] E. Lara-Curzio, (SECA) Core Technology Peer Review Workshop, Tampa, FL, USA, 2005.
[57] K. Tanaka, Y. Akiniwa, H. Kimura, K. Ukai, M. Yokoyama, Y. Mizutani, Mater. Sci. Forum 571–572 (2008) 339–344.
[58] J. Malzbender, R.W. Steinbrech, J. Power Sources 173 (2007) 60–67.
[59] J. Laurencin, G. Delette, M. Dupeux, F. Lefebvre-Joud, ECS Trans. 7 (2007) 677–686.
[60] J. Malzbender, R.W. Steinbrech, Surf. Coat. Technol. 176 (2004) 165–172.
[61] A. Selcuk, A. Atkinson, J. Am. Ceram. Soc. 83 (2000) 2029–2035.
[62] J. Malzbender, R.W. Steinbrech, J. Eur. Ceram. Soc. 28 (2008) 247–252.
[63] E. Ivers-Tiffée, H. Timmermann, A. Leonide, N.H. Menzler, J. Malzbender, in: W. Vielstich, H.A. Gasteiger, H. Yokokawa (Eds.), Handbook of Fuel Cells—Fundamentals, Technology and Applications, Volume 5: Advances in Electrocatalysis, Materials, Diagnostics and Durability, John Wiley & Sons Ltd., Chichester, England, 2009, pp. 933–956.
[64] A. Weber, A.C. Müller, D. Herbstritt, E. Ivers-Tiffée, in: H. Yokokawa, S.C. Singhal (Eds.), Proceedings of the VIIth Int. Conf. on Solid Oxide Fuel Cells, Tsukuba, Japan, 2001, pp. 952–962.
[65] E. Ivers-Tiffée, W. Wersing, H. Greiner, in: R. Waser (Ed.), Electroceramics IV: Electroceramics and Applications I–III, 1994, p. 1.
[66] R.W. Jackson, J.P. Leonard, F.S. Pettit, G.H. Meier, Solid-State Ionics 179 (2008) 2111–2120.